Article ID: 1000-7032(2012)07-0774-06

Design of Active Region for Watt-level VCSEL at 1 060 nm

ZHANG Li-sen[1,2], NING Yong-qiang[1*], ZENG Yu-gang[1], ZHANG Yan[1,2], QIN Li[1], LIU Yun[1], WANG Li-jun[1], CAO Jun-sheng[1], LIANG Xue-mei[3]

(1. *State Key Laboratory of Luminescence and Application, Changchun Institute of Optics, Fine Mechanics and Physics, Chinese Academy of Sciences, Changchun* 130033, *China*;
2. *Graduate University of the Chinese Academy of Sciences, Beijing* 100039, *China*;
3. *Institute of Information Technology, Jilin Agricultural University, Changchun* 130033, *China*)
* *Corresponding Author, E-mail: ningyq@ciomp.ac.cn*

Abstract: The active region of high power VCSEL at 1 060 nm is calculated and designed. The performances of highly-strained InGaAs quantum wells with GaAsP, GaAs and AlGaAs barriers are compared. A comprehensive model taking self-heating effect into consideration is presented to determine the parameters of quantum well and barrier. It is found that the best value of width and number of $In_{0.28}Ga_{0.72}As$ quantum wells in our design is 9 nm and 3, respectively. And high output power up to Watt-level is achieved. In addition, the temperature performances are also compared among the three different barriers, which show that the devices with GaAsP barriers have higher output power and better temperature stability. Finally, the InGaAs/GaAsP QWs are grown used MOCVD and the PL spectrum is tested, the experimental data agrees with the theoretical results very well.

Key words: vertical-cavity surface-emitting laser; 1 060 nm; Watt-level; InGaAs
CLC number: TN248.4 **Document code**: A **DOI**: 10.3788/fgxb20123307.0774

1 060 nm高功率垂直腔面发射激光器的有源区设计

张立森[1,2], 宁永强[1*], 曾玉刚[1], 张 艳[1,2],
秦 莉[1], 刘 云[1], 王立军[1], 曹军胜[1], 梁雪梅[3]

(1. 发光学及应用国家重点实验室 中国科学院长春光学精密机械与物理研究所, 吉林 长春 130033;
2. 中国科学院 研究生院, 北京 100039; 3. 吉林农业大学 信息技术学院, 吉林 长春 130033)

摘要: 对1 060 nm高功率垂直腔面发射激光器的有源区进行了理论计算和设计。对比了GaAsP、GaAs和AlGaAs三种不同材料的垒层所组成的高应变InGaAs量子阱的性能。为了确定有源区阱层和垒层的参数,考虑了自热效应对功率的影响,使得模型更加精确可靠。发现所设计的$In_{0.28}Ga_{0.72}As$量子阱的阱宽和阱数的最佳值分别为9 nm和3个,输出功率可以达到瓦级。另外,对比了三种不同垒层的温度特性,结果显示,使用GaAsP垒层的器件在高温下具有更高的功率和更好的温度稳定性。最后,利用MOCVD生长了InGaAs/GaAsP量子阱并测试了其PL谱,实验数据与理论结果符合得很好。

关 键 词: 垂直腔面发射激光器; 1 060 nm; 瓦级; InGaAs

收稿日期: 2011-04-13; **修订日期**: 2011-05-23
基金项目: 国家自然科学基金(10974012,11074247,61106047,61176045,61106068,51172225,61006054); 国家自然科学基金重点(90923037)资助项目
作者简介: 张立森(1985-), 男, 山东聊城人, 主要从事高功率垂直腔面发射激光器的研究。
E-mail: zhls1209@163.com, Tel: (0431)86176335

1 Introduction

High-power laser at 1 060 nm wavelength, *e. g.* Nd: YAG, has very wide applications. It can be used in the scientific, medical and industrial laser systems such as laser marking, laser drilling and other laser material processing systems. Due to the compact structure of vertical-cavity surface-emitting laser (VCSEL)[1-3], it is a promising alternative to solid-state Nd: YAG lasers. In addition, green laser can be realized through intra-cavity frequency doubling by fabricating vertical-external-cavity surface-emitting laser (VECSEL)[4].

At present, the research of VCSEL at 1 060 nm focuses on devices with small output power which are used in optical interconnection[5-6]. The maximum slope efficiency and power conversion efficiency of 1 W/A and 62% are obtained from a double intra-cavity structure. However, in order to get higher power at 1 060 nm, large aperture of hundreds of micrometers is needed where the double intra-cavity structure can not used. And the self-heating effect must be considered, which greatly influences the output power of devices. There is little investigation on high power VCSEL at 1 060 nm, so it is significant to research theoretically on the devices.

In this paper, the active region of 1 060 nm VCSEL is calculated and designed theoretically. The composition of indium and the width of quantum well are optimized to obtain best performance. In addition, the characteristics of devices with GaAsP, AlGaAs and GaAs barriers are also compared. Finally, the InGaAs/GaAsP QWs are grown used MOCVD and the PL spectrum is tested.

2 Experiments

2.1 Calculation of Bandgap

The expression of the strain is

$$\varepsilon = \frac{a_0 - a}{a}, \tag{1}$$

where a is the lattice constant of the epitaxial layer and a_0 is the lattice constant of the substrate. The shift of the conduction band and valence band due to the strain effects is

$$\delta E_c(x) = 2a_c\left(1 - \frac{C_{12}}{C_{11}}\right)\varepsilon, \tag{2}$$

$$\delta E_v(x) = 2a_v\left(1 - \frac{C_{12}}{C_{11}}\right)\varepsilon \pm b\left(1 + 2\frac{C_{12}}{C_{11}}\right)\varepsilon, \tag{3}$$

where a_c and a_v are the conduction band and valence band hydrostatic deformation potential, b is the valence band shear deformation potential, C_{11} and C_{12} are the elastic stiffness constant of materials, and the sign of "+" and "−" is corresponding to the band of the heavy hole and the light hole, respectively.

Then the strained bandgap of bulk material can be expressed as

$$E_g(x) = E_g^0(x) + \delta E_c(x) - \delta E_v(x), \tag{4}$$

where $E_g^0(x)$ is the unstrained bandgap.

The bandgap of quantum well is written as

$$\frac{hc}{\lambda} = E_{c1-h1} = E_g + E_{c1} + E_{h1}. \tag{5}$$

2.2 Characteristics of Device

For VCSELs with quantum well active layer, the threshold current can be written as[7]

$$I_{th} = qn_w L_w B_{eff} N_{tr}^2 \pi r^2 / \eta_i \cdot \exp\left[\frac{2}{a_N \Gamma}\left(\alpha_{in} + \frac{1}{L_{eff}}\ln\frac{1}{\sqrt{R_t R_b}}\right)\right], \tag{6}$$

$$\Gamma = \frac{\int_{QWs} E^2(z)\,dz}{\int_{L_{eff}} E^2(z)\,dz}, \tag{7}$$

where q is the quantity of electronic charge, n_w and L_w are the number and width of QWs respectively, B_{eff} is the effective recombination constant, N_{tr} is the carrier concentration at transparency, r is the radius of VCSEL, η_i is the internal quantum efficiency, a_N is the gain coefficient, Γ is the confinement factor, $E(z)$ is the electric field intensity, L_{eff} is the effective length of the cavity, α_{in} is the total internal loss, R_t and R_b are respectively the reflectivities of the top and bottom DBRs.

The output power of the VCSEL considering the effect of temperature can be calculated using the following expressions[7]:

$$P = \eta_i \frac{\lg(1/\sqrt{R_t R_b})}{\alpha_{in} L_{eff} + \lg(1/\sqrt{R_t R_b})} \frac{h\nu}{q}(I - I_{th})\left(1 - \frac{\Delta T}{T_{off}}\right), \tag{8}$$

$$\Delta T = R_T[(V_0 + IR_d)I - P], \tag{9}$$

where $R_T = (4\lambda_c r)^{-1}$ is the thermal resistance, λ_c is the average thermal conductivity, h and ν are respectively the Plank constant and the photon frequency, I is the injection current, V_0 is the turn-on voltage, R_d is the series resistance, T_{off} is the cut-off temperature.

3 Results and Discussion

The material parameters of the ternary semiconductors can be obtained through a linear interpolation between the parameters of the binary semiconductors[8]. The relevant material parameters are listed in Table 1[8], where, a is lattice constant, C_{11} and C_{12} are elastic stiffness constants, a_c is hydrostatic deformation potential for conduction band, a_v is hydrostatic deformation potential for valence band, b is shear deformation potential for valence band, respectively.

Table 1 Parameters of some binary material systems

Material	a/nm	C_{11}/(10^6 N·cm^{-2})	C_{12}/(10^6 N·cm^{-2})	a_c/eV	a_v/eV	b/eV
GaAs	0.565 33	11.879	5.376	−7.17	1.16	−1.7
InAs	0.605 84	8.329	4.526	−5.08	1.00	−1.8
GaP	0.545 05	14.05	6.203	−7.14	1.70	−1.8

In order to obtain the parameters of QWs, the bandgap of InGaAs, GaAsP and AlGaAs are calculated and shown in Fig. 1. It can be seen that the bandgap of strained-heavy hole is smaller than the value of strained-light hole in InGaAs material. So the transition happens mainly between the conduction band and the heavy hole band. The $GaAs_{0.8}P_{0.2}$ and $Al_{0.15}Ga_{0.85}As$ layers are used as barriers to confine carriers better.

Fig. 2 presents the dependence of bandgap and wavelength on the well width at different composition of In, respectively. The In composition and the well width can be selected from different combinations according to Fig. 2. To get the best parameters of QWs, the output characteristics should be calculated and compared. The parameters used are listed in Table 2, where, B_{eff} is effective recombination constant, η_i is internal quantum efficiency, L_{eff} is effective

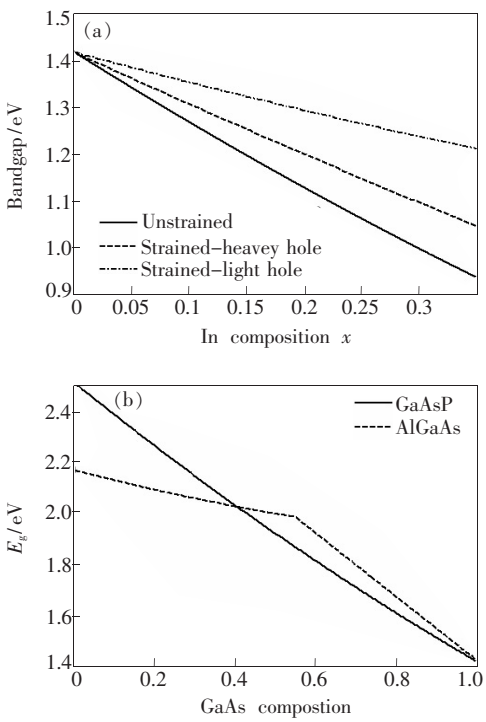

Fig. 1 The bandgap of (a) unstrained and strained InGaAs material and (b) GaAsP and AlGaAs material

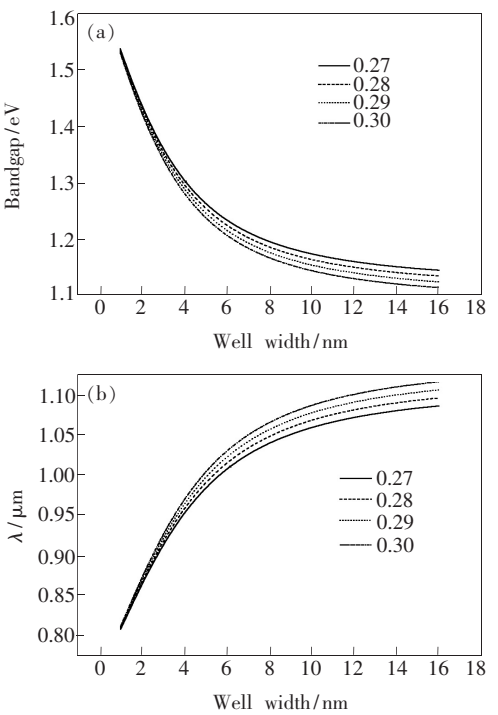

Fig. 2 The dependence of (a) bandgap and (b) wavelength on the well width with different In composition

Table 2　Material and structural parameters

$B_{eff}/(cm^3 \cdot s^{-1})$	$\eta_i/\%$	L_{eff}/nm	α_{in}/cm^{-1}	V_0/V	R_d/Ω	$T_{off}/℃$
1.5×10^{-10}	100	1 130	10	1.4	0.1	170

cavity length, α_{in} is Total internal loss, V_0 is turn-on voltage, R_d is series resistance, T_{off} is cut-off temperature, respectively.

The transparency carrier density and the gain coefficient are obtained by curve-fitting to the peak gain of materials, which are listed in Table 3.

Table 3　Transparency carrier density and gain coefficient at different well width

Well width/nm	$a_N/(10^{17}\ cm^{-3})$	g_{tr}/cm^{-1}
7	9.73	2 802
8	8.85	2 439
9	7.77	2 065
10	7.98	1 876

Fig. 3 shows the dependent of threshold current on the number of QWs. The threshold current decreases sharply and then increases slowly with the increase of the number of QWs. And the lowest value happens when the number is 3, which is used in our design. The output power is compared in Fig. 4 for $In_xGa_{1-x}As$ QWs with different In composition from 0.27 to 0.30, and the corresponding well width is 10,9,7,6 nm, respectively. These parameters are selected in order to get the certain wavelength of around 1 050 nm which is determined by considering the different rates shifting to longer wavelength between the gain peak and the cavity mode with the increase of temperature. The maximum power and the minimum threshold current are got for the well

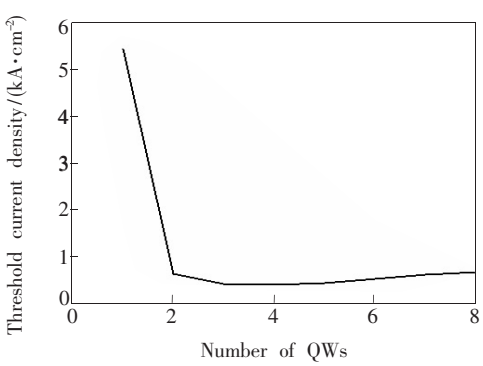

Fig. 3　The dependence of the threshold current density on the number of QWs

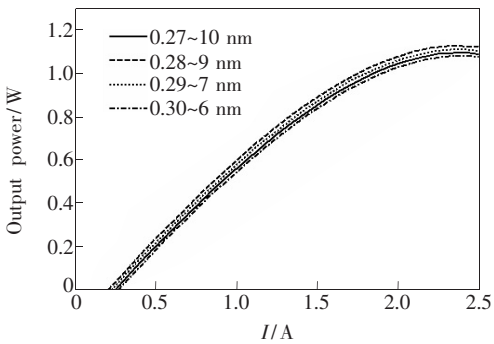

Fig. 4　The output power versus current at different In composition

width of 9 nm and the In composition of 0.28.

In order to measure the temperature characteristic, the performances of devices with the tensile strained $GaAs_{0.8}P_{0.2}$ barrier and unstrained barriers of GaAs and $Al_{0.15}Ga_{0.85}As$ are compared. Fig. 5 presents the peak gain versus temperature for $GaAs_{0.8}P_{0.2}$, GaAs, and $Al_{0.15}Ga_{0.85}As$, respectively. It can be seen that the QWs with $Al_{0.15}Ga_{0.85}As$ and GaAs barriers have higher peak gain than the QW with $GaAs_{0.8}P_{0.2}$ barrier at lower temperature, but the peak gain for $GaAs_{0.8}P_{0.2}$ barrier decreases slower with the increase of temperature than that of the other two barriers. It is concluded that the ten sile strained $GaAs_{0.8}P_{0.2}$ barrier has more highly stability with the temperature increasing from 273 K to 500 K.

To improve the conclusion above, the output performances for the three different barriers are studied. The output power versus current at 325 K and 350 K

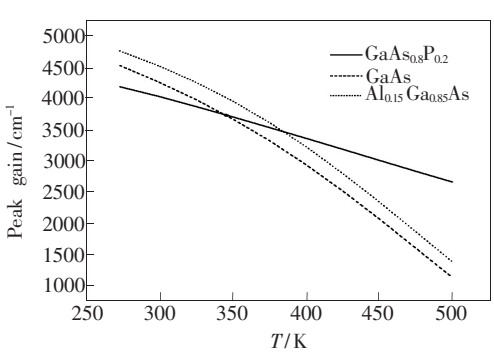

Fig. 5　The peak gain versus temperature for GaAsP, GaAs, and AlGaAs barriers.

is shown in Fig. 6 (a) and (b), respectively. The performances of the three barriers become worse when the temperature arises. The $GaAs_{0.8}P_{0.2}$ barrier has the lowest threshold current and the highest output power at high temperatures. The decrease rate of the output power of $GaAs_{0.8}P_{0.2}$ barrier is the slower than the other two barriers, which means that the QWs with the $GaAs_{0.8}P_{0.2}$ barrier have better high-temperature performance which is agreed with the conclusion above. The maximum output power larger than 1 W can be achieved.

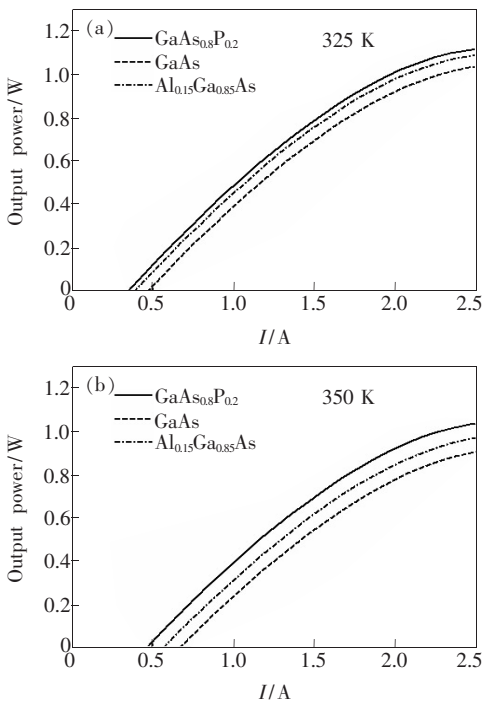

Fig. 6 The output power versus current for the three different barriers at (a) 325 K and (b) 350 K, respectively.

As the $In_{0.28}Ga_{0.72}As$ QWs is compressive strained, the critical thickness must be considered[9]. Fig. 7 shows the critical thickness of InGaAs with different In composition grown on GaAs substrate. We can see that the critical thickniss of $In_{0.28}Ga_{0.72}As$ material is less than 10 nm, it is hard to achieve high crystal quality for the unstrained GaAs and $Al_{0.15}Ga_{0.85}As$ barriers when the number of QWs is more than one. Different from this situation, the $GaAs_{0.8}P_{0.2}$ barrier is tensile strained which is opposite to the strain of the well layer. By introducing a strain-compensated barrier into the active region, it is possible to make the net strain be equal to zero, which leads

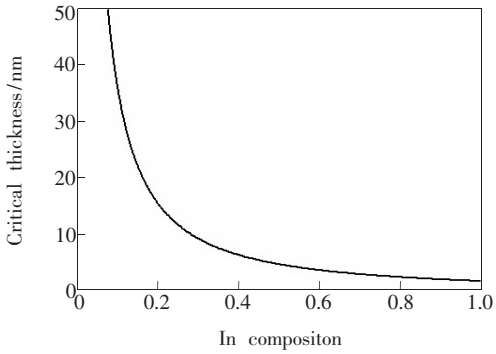

Fig. 7 The critical thickness of InGaAs with different In composition grown on GaAs substrate

to better crystal quality free of misfit dislocations. And larger mode gain and higher power can be obtained from devices with a large number of QWs. For this reason, the $GaAs_{0.8}P_{0.2}$ is also the better barrier for the $In_{0.28}Ga_{0.72}As$ QWs.

In order to verify the correctness of the above design, the lasing spectrum of VCSEL is simulated using PICS3D software, the $In_{0.28}Ga_{0.72}As/GaAs_{0.8}P_{0.2}$ QWs are grown with MOCVD and the PL spectrum is tested, which are shown in Fig. 8. Both the center wavelength of lasing spectrum and the peak wavelength of the PL spectrum are around 1 050 nm, which is designed considering the shift with the

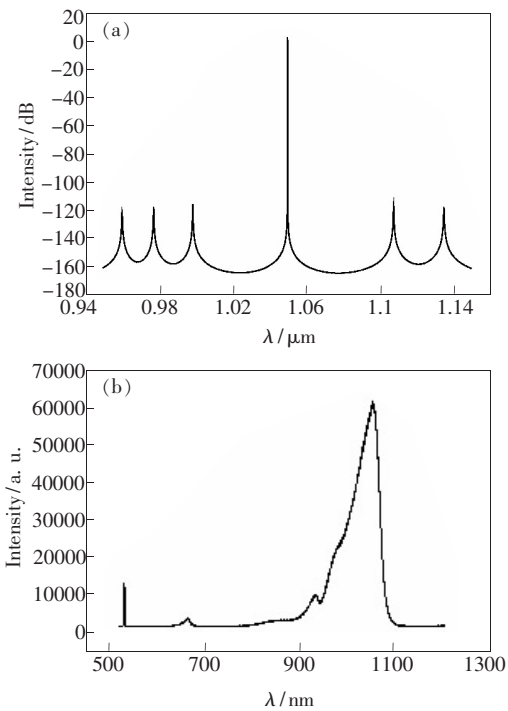

Fig. 8 (a) The lasing spectrum of VCSEL, and (b) PL spectrum of $In_{0.28}Ga_{0.72}As/GaAs_{0.8}P_{0.2}$ QWs.

increase of temperature. The experimental data agrees with the theoretical results very well.

4 Conclusion

The active region of high power VCSEL at 1 060 nm is calculated and designed theoretically taking self-heating effect into consideration. The performance of different In composition and width of quantum well are calculated. It is found that the best value of width and number of quantum wells in our design is 9 nm and 3, respectively. In addition, the characteristics of devices with GaAsP, AlGaAs and GaAs barriers are also compared. The QWs with $GaAs_{0.8}P_{0.2}$ barrier show better temperature stability. And high power more than 1 W is achieved from VCSELs with three $In_{0.28}Ga_{0.72}As/GaAs_{0.8}P_{0.2}$ quantum wells. Finally, the $In_{0.28}Ga_{0.72}As/GaAs_{0.8}P_{0.2}$ QWs are grown used MOCVD and the peak wavelength of PL spectrum is around 1 050 nm, which is satisfied with the design requirement.

References:

[1] Zhang Y, Ning Y Q, Qin L, *et al*. Design and fabrication of vertical-cavity surface-emitting laser with small divergence [J]. *Chin. J. Lumin.* (发光学报), 2011, 32(1):47-52 (in Chinese).

[2] Shi J J, Qin L, Ning Y Q, *et al*. Coherent measurement and analysis of vertical-cavity surface-emitting laser [J]. *Chin. J. Lumin.* (发光学报), 2011, 32(8):834-838 (in Chinese).

[3] Wang Z F, Ning Y Q, Zhang Y, *et al*. High power and good beam quality of two-dimensional VCSEL array with integrated GaAs microlens array [J]. *Opt. Express*, 2010, 18(23):23900-1-6.

[4] Shchegrov A V, Umbrasas A, Watson J P, *et al*. 532 nm laser sources based on intracavity frequency doubling of extended cavity surface-emitting diode lasers [J]. *SPIE*, 2004, 5332:151-156.

[5] Hou H Q, Choquette K D, Geib K M, *et al*. High-performance 1.06-μm selectively oxidized vertical-cavity surface-emitting lasers with InGaAs-GaAsP strain-compensated quantum wells [J]. *IEEE Photonics Technol. Lett.*, 1997, 9(8):1057-1059.

[6] Hatakeyama H, Anan T, Akagawa T, *et al*. Highly reliable high-speed 1.1-μm-range VCSELs With InGaAs/GaAsP-MQWs [J]. *IEEE J. Quantum Electron.*, 2010, 46(6):890-897.

[7] Yu S F. *Analysis and Design of Vertical Cavity Surface Emitting Laser* [M]. Hoboken: Wiley-Interscience, 2003:47-82.

[8] Minch J, Park S H, Keating T, *et al*. Theory and experiment of $In_{1-x}Ga_xAs_yP_{1-y}$ and $In_{1-x-y}Ga_xAl_yAs$ long-wavelength strained quantum-well lasers [J]. *IEEE J. Quantum Electron.*, 1999, 35(5):771-782.

[9] Matthews J W, Blakeslee A E. Defects in epitaxial multilayers: I. Misfit dislocations [J]. *J. Crystal Growth*, 1974, 27(1):118-125.